Astronomy & Astrophysics manuscript no. article˙astroph
February 5, 2008

Numerical simulations of coronal magnetic field loop evolution

T.G. Yelenina,[1] G.V. Ustyugova[1] and A.V. Koldoba[2]

[1] Keldysh Institute for Applied Mathematics (KIAM), Russian Academy of Sciences, Miusskaya square 4, 125047 Moscow, Russia
e-mail: elen@keldysh.ru ; e-mail: ustyugg@rambler.ru
[2] Institute of Mathematical Modelling (IMM), Russian Academy of Sciences, Miusskaya square 4a, 125047 Moscow, Russia
e-mail: koldoba@spp.keldysh.ru

will be inserted by hand later

ABSTRACT

Aims. We present the results of the numerical simulations of the interaction between a magnetized star and an imperfectly conducting accretion disk.
Methods. To analyze the "star–disk" interaction we numerically investigate the MHD equations used Godunov-type high resolution numerical method.
Results. It was found that the "star – disk" interaction occurs with quasi-periodic reconnection of the magnetic field coronal loops and plasmoid ejections. In the case of the perfect disk conductivity the evolution of the coronal magnetic field leads to the periodic outflow of angular momentum from the disk. In the case of an imperfectly conducting disk the configuration of the magnetic field is formed such that the disk angular momentum carried by magnetic field gets balanced by angular momentum carried by matter.

Key words. Magnetohydrodynamics (MHD) – accretion disks – stars: magnetic field – interstellar medium: evolution – methods: numerical

1. Introduction

This paper studies the evolution of the coronal magnetic field linked with a magnetized star and its accretion disk. We suggest that the plasma differential rotation along magnetic field lines is the reason of a "star–corona–disk" system evolution. We suppose that the magnetic field lines are frozen in the perfectly conducting coronal plasma. The differential rotation leads to the generation of the magnetic field toroidal component. Magnetic pressure increases in corona inner part and plasma is pushed towards the outer part together with the magnetic field lines. As a result there is deformation or even opening of poloidal magnetic field lines adopting a new configuration. The type of this new configuration is determined by several factors. One of them is the electrical conductivity of the relatively cold disk plasma.

We assume in this model that the imperfect plasma conductivity is essential only in the disk and is determined by velocity turbulent fluctuations. The value of the turbulent magnetic diffusivity we consider as a free parameter of the problem. To obtain an acceptable range for this parameter, it is supposed that the coefficient of the turbulent magnetic diffusivity agrees in order of magnitude with the turbulent viscosity accepted in the standard α-model of Shakura–Sunyaev accretion disk (Shakura & Sunyaev 1973).

Send offprint requests to: T.G. Yelenina e-mail: elen@keldysh.ru

We consider that the disk is formed by relatively dense and cold matter. The disk is Keplerian and sound speed is much less than the Keplerian one. It means that disk is geometrically thin. In this model, the disk is considered as an infinitely thin, conductive plane. It should be mentioned that disk has a complicated structure and its interaction with the magnetic field does not reduce to magnetic compression and magnetic field lines slippage relatively to matter (Balbus et al. 1995).

Besides the dynamics of the magnetic field, it is worthy to know its configuration after the opening of the magnetic field lines. This configuration defines the disk and the magnetic field evolution at large time scales. The main factor influencing this evolution is the rate of angular momentum transfer from the disk. The important role in this process belongs also to the magnetic field (Ferreira 1997).

A sufficiently strong magnetic field can lead also to the formation of a matter outflow from the disk to the corona. In case of a thin Keplerian disk, a criterion for the "wind" formation beginning has been given by Blandford & Payne (1982). To generate this outflow from a Keplerian disk, the magnetic field line should be inclined to the rotation axis with an angle of more than 30°. In that case a magnetic field line plays the role of a "rail" along which matter leaves the disk. Thus the final magnetic field configuration determines strongly both the rate of disk accretion, through the rate of angular momentum out-

flow, and the rate of matter outflow along the magnetic field lines inclined to the rotation axis.

There are lots of papers concerning the evolution of the magnetic field in interaction with a disk. We would like to mention some of them. Hayashi et al. (1996) presented resistive MHD simulations with diffusive accretion disk and dipole stellar magnetic field topology. Kuwabara et al. (2000) introduced resistivity to simulate the effects of turbulent magnetic diffusivity. Romanova et al. (2002) studied the disk accretion to a rotating magnetized star with an aligned dipole moment and associated funnel flows, they described the "star–disk" interaction for the cases of fast and slowly rotating star. These simulations included a treatment of the disk vertical structure. Some papers presented the results of ideal MHD simulations considered the disk like a boundary condition. Ustyugova et al. (1999) for initially split-monopole magnetic field configuration, Ouyed & Pudritz (1997) for dipole topology, Krasnopolsky et al. (1999) studied MHD outflows from the disk. Fendt & Elstner (1999, 2000) studied the "star–disk" interaction, they observed the opening of magnetic field lines and outflows. Fendt & Čemeljić (2002) studied the jet formation and propagation by used the resistive MHD equations.

Shu et al. (1994) presented steady state dynamics of accretion from viscous and imperfectly conducting disk. Ferreira (1997) gave self-similar solution for the resistive disk for stationary MHD equations. Uzdensky (2004) gave a review of modern theoretical scenario of the star–disk system interaction, including both stationary and time-dependent ones.

In this paper we consider the evolution of the magnetic field configuration from an initial dipole-like topology into the final one. We analyze the time-dependent ideal MHD equations using the high resolution Godunov-type method. We consider for a setup model of "star–disk" system that the generated flow is axisymmetric and symmetric in relation with the equatorial plane. The dependence of the disk angular momentum outflow rate on the disk surface electrical conductivity is investigated.

The structure of the paper is as follows. After the introduction we propose the model and the evaluation of the disk surface magnetic diffusivity. Then we present the numerical method and describe our results for number disk surface magnetic diffusivity. Finally we formulate the main conclusions.

2. Statement of the problem

Let us consider a "star–corona–disk" system governed by the magnetic field (see Fig. 1). In our model the star has mass M_*, magnetic moment μ_* and angular velocity Ω_*. It is assumed that the star rotation axis aligns with its magnetic axis z. The disk rotating around the star is considered to be infinitely thin and located at $z = 0$. It is supposed that the disk is rotating following Keplerian orbits around the star and the disk is imperfectly conducting. The particle velocity in a Keplerian orbit with radius r is $V_\mathrm{k} = \sqrt{GM_*/r}$, where $G = 0.667 \cdot 10^{-7}\mathrm{cm^3 g^{-1} sec^{-2}}$ is gravitational constant. Thus, the disk is differentially rotating.

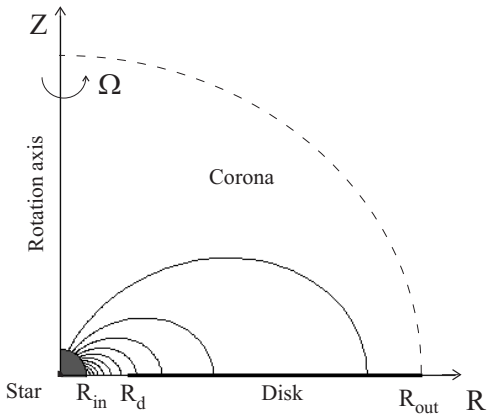

Fig. 1. Sketch of a magnetically linked "star–disk" system. The solid lines show the magnetic field lines. R_in, R_out are the edges of the computational domain. The star is inside the computational domain, $R_* < R_\mathrm{in}$.

The coronal plasma electro-conductivity is big enough, so we can describe the flow by the system of the ideal MHD equations

$$
\begin{aligned}
&\frac{\partial \rho}{\partial t} + \nabla \cdot (\rho \boldsymbol{u}) = 0,\\
&\frac{\partial \rho \boldsymbol{u}}{\partial t} + \nabla \mathsf{T} = \rho \boldsymbol{g},\\
&\frac{\partial \boldsymbol{B}}{\partial t} - \nabla \times (\boldsymbol{u} \times \boldsymbol{B}) = 0,\\
&\frac{\partial \rho S}{\partial t} + \nabla \cdot (\rho S \boldsymbol{u}) = 0,\\
&\nabla \boldsymbol{B} = 0.
\end{aligned}
\qquad (1)
$$

Here $\mathsf{T}_{ik} = \rho u_i u_k + p\,\delta_{ik} + \frac{1}{4\pi}\left(-B_i B_k + \frac{B^2}{2}\delta_{ik}\right)$ is the stress tensor; $\boldsymbol{u}$ is the plasma velocity; $\boldsymbol{B}$ is the magnetic field; ρ and p are the plasma density and pressure; $S = p/\rho^\gamma$ is the entropy function; γ is the adiabatic index; $\boldsymbol{g} = -\nabla\Phi_\mathrm{g}$ is the gravitational acceleration; $\Phi_\mathrm{g} = -GM_*/R$ is the star gravity potential; R is the distance from the gravitating center.

The system (1) is solved in spherical coordinates (R, φ, θ), with θ being the polar angle with the symmetry axis. Velocity $\boldsymbol{u}$ and magnetic field $\boldsymbol{B}$ have all their components $\boldsymbol{u} = (u, v, w)$ and $\boldsymbol{B} = (B_R, B_\varphi, B_\theta)$.

The aim of this paper is to investigate the character of the magnetic field evolution and field topology depending on the disk surface magnetic diffusivity $\zeta = c^2/2\pi\lambda$ (λ is surface electric conductivity, c is the speed of light) at large time scales. As it will be shown below, it used in boundary conditions set on the equatorial plane $z = 0$.

2.1. Dimensionless variables and typical quantities for T Tauri stars

The dimensionless form of (1) is received in standard way. As distance scale, R_0, we take one third of the distance from the star center to the inner edge of the disk. Thus, in dimensionless units the disk inner edge is $R_\mathrm{d} = 3R_\mathrm{in}$. The inner radius of the computational domain in dimensionless units is $R_\mathrm{in} = 1$. The time and the velocity scales are chosen that in dimensionless units $GM_* = 1$. This requirement yields $t_0 = \sqrt{R_0^3/GM_*}$ as the time scale and $v_0 = R_0/t_0$ as the velocity scale. As a magnetic field scale, B_0 is taken and then density, pressure and magnetic moment scales are $\rho_0 = B_0^2/v_0^2$, $p_0 = B_0^2$, $\mu_{*0} = B_0R_0^3$.

As typical quantities of T Tauri stars we adopt standard values like a star mass $M_* = 0.8M_\odot = 1.6 \cdot 10^{33}$ g, and $R_d = 9R_\odot = 5.4 \cdot 10^{11}$ cm. Therefore the distance scale is $R_0 = R_\mathrm{d}/3 = 1.8 \cdot 10^{11}$ cm, the time and velocity scales are $0.74 \cdot 10^4$ s and $2.43 \cdot 10^7$ cm s^{-1} respectively. The Keplerian rotation period at the disk inner edge is 8.3 days. The simulation region size is $1.134 \cdot 10^{12}$ cm.

The star magnetic moment is taken such that the magnetic field on the star surface is 300 G, so $B_0 = 6.5$ G. Thus, on the disk inner part, the dipole magnetic field is 2.4 G, $R_* = 3/5R_\mathrm{in}$, $\mu_* = 10$ and the magnetic moment is $3.8 \cdot 10^{35}$G cm^3. The density scale is $1.44 \cdot 10^{-14}$g cm^{-3}, typical for the disks around T Tauri stars.

2.2. Evaluation of the electric conductivity in the disk

We suggest that turbulent diffusion of magnetic field is determined by the same processes that determine turbulent viscosity, which leads to angular momentum transport in the disk. Thus, it is assumed that turbulent magnetic diffusivity η_t is in the order of turbulent viscosity like in the Shakura–Sunyaev model (Shakura & Sunyaev 1973): $\eta_\mathrm{t} = \alpha_\mathrm{t} c_\mathrm{s} h$, where c_s is the sound speed in the disk, h is the disk half-thickness, α_t is the dimensionless coefficient varying, according to Balbus (2003), in this range $0.01 \div 0.6$.

Under hydrostatic equilibrium, the Keplerian disk half-thickness h can be found from the relation: $(h/r)^2 + b(h/r) - (c_\mathrm{s}/V_\mathrm{k})^2 = 0$, where $b \equiv r(B_r^2 + B_\varphi^2)/(4\pi\Sigma V_\mathrm{k}^2)$, Σ is the surface density, V_k is Keplerian velocity, B_r, B_φ are the magnetic field components (Bisnovatyi–Kogan & Lovelace 2001). In any case, even without taking into account the magnetic compression, the disk half-thickness satisfies the inequality $h \lesssim c_\mathrm{s}/\Omega_k$, where Ω_k is Keplerian angular velocity. Therefore, the turbulent magnetic diffusivity becomes $\eta_\mathrm{t} \lesssim \alpha_\mathrm{t} c_\mathrm{s}^2/\Omega_\mathrm{k}$.

The sound speed is much less than the Keplerian one is due to the disk is cold. It means that $h \lesssim c_\mathrm{s}/\Omega_\mathrm{k} \ll r$, i.e. disk is geometrically thin. In this model, the disk is considered as an infinitely thin, conductive plane.

The turbulent electro-conductivity $\sigma_\mathrm{t} = c^2/(4\pi\eta_\mathrm{t}) = c^2/(4\pi\alpha_\mathrm{t} c_\mathrm{s} h)$ is associated with the magnetic diffusivity η_t. The surface disk conductivity is $\lambda = \int \sigma_\mathrm{t} dz \sim 2h\sigma_\mathrm{t} = c^2/(2\pi\alpha_\mathrm{t} c_\mathrm{s})$, and the surface magnetic diffusivity is

$$\zeta = \frac{c^2}{2\pi\lambda} = \alpha_\mathrm{t} c_\mathrm{s} = \alpha_\mathrm{t}\left(\frac{c_\mathrm{s}}{V_\mathrm{k}}\right) V_\mathrm{k}.$$

In thin accretion disks $c_\mathrm{s}/V_\mathrm{k} = h/r \ll 1$. Thus, an acceptable coefficient of the magnetic surface diffusivity is $\zeta = (0.01 \div 0.6)(c_\mathrm{s}/V_\mathrm{k})V_\mathrm{k}$.

2.3. Initial conditions

We suggest that, at the initial time, the stellar magnetic field with dipole-like topology and magnetic moment μ_* penetrates the corona and the disk. So, the components of the magnetic field $\boldsymbol{B}$ are

$$B_R = \frac{2\mu_* \cos\theta}{R^3},\ B_\theta = \frac{\mu_* \sin\theta}{R^3},\ B_\varphi = 0.$$

We suppose that at the initial time $t = 0$, the matter of the corona and the disk is in mechanical equilibrium with the force-free dipole magnetic field, i.e. gravitational force is balanced with "centrifugal" force (liquid particle acceleration) and pressure gradient.

The momentum equation for the system (1) taking into account that particles follow circular orbits is

$$-\omega^2 r\boldsymbol{e}_r + \frac{1}{\rho}\nabla p = -\nabla\Phi_g, \tag{2}$$

where $\boldsymbol{e}_\mathrm{r}$ is a unit vector with the direction of the cylindrical radius $r = R\sin\theta$, that on disk surface it is $\theta = \pi/2$ and $r = R$.

This is due to the magnetic pressure $\boldsymbol{B}^2/8\pi$ of the dipole-like field $\boldsymbol{B}$ decreases like $1/R^6$. Also, the most of the simulation region is occupied by a relatively dense plasma, where gas pressure dominates. This dense plasma prevents opening of the magnetic field lines. Let us consider that density ρ is function not only of pressure p but also of cylindrical radius r: $\rho = \rho(r, p)$. Let us denote $V(p, r) = 1/\rho$. The momentum equation along the z axis (the projection of equation (2) to the z axis) is

$$V(p, r)\frac{\partial p}{\partial z} + \frac{\partial\Phi_g}{\partial z} = 0.$$

Integrating it by z and suggested that $p \to 0$ under $z \to \infty$ and $\Phi_g \to 0$) we finally get that

$$\int_0^p V(p', r)dp' + \Phi_g = 0. \tag{3}$$

The integral is assumed to converge on its interior limit.

Let us consider now the momentum equation (2) along the radial direction

$$-\omega^2 r + V(p, r)\frac{\partial p}{\partial r} + \frac{\partial\Phi_\mathrm{g}}{\partial r} = 0, \tag{4}$$

After differentiating equation (3) by r and subtracting (4) from it we get

$$\omega^2 r + \int_0^p \frac{\partial V}{\partial r}dp' = 0. \tag{5}$$

Thus, given the function $V(p, r)$, the relation (3) defines the function $p\,(r, z)$ and relation (5) – function $\omega(r, z)$.

If $V(p,r) = k(r)/p^{\alpha}$, $\alpha = \text{const} < 1$ (this condition is essential for the convergence of the integral in left part of equation (3) as $p \to 0$), then equations (3), (5) take the form

$$\begin{cases} \dfrac{kp^{1-\alpha}}{1-\alpha} + \Phi_g = 0, \\ \dfrac{p^{1-\alpha}}{1-\alpha} k' + \omega^2 r = 0. \end{cases}$$

Integrating it, we found the function $k(r)$

$$\ln k = -\frac{1}{GM_*} \int \Omega^2(r) r^2 dr. \tag{6}$$

Here $\Omega(r) = \omega(r,0)$ is the angular velocity at equatorial plane $z = 0$.

The angular velocity at the equatorial plane was chosen in the following way (r_1, r_2 are the parameters of the problem and $r_1 = 2R_{\rm in}$, $r_2 = 3R_{\rm in}$):

$$\Omega(r) = \begin{cases} \Omega_* = \sqrt{GM_*/r_1^3}, & 0 < r < r_1, \\ \Omega_* + \dfrac{\sqrt{GM_*/r_2^3} - \Omega_*}{r_2 - r_1}(r - r_1), & r_1 < r < r_2, \\ \sqrt{GM_*/r^3}, & r > r_2. \end{cases} \tag{7}$$

As a result, the distributions of the pressure $p(r,z)$, density $\rho(r,z)$ and angular velocity $\omega(r,z)$ are obtained

$$p(r,z) = \left(\frac{1-\alpha}{k(r)} \frac{GM_*}{\sqrt{r^2+z^2}} \right)^{1/(1-\alpha)}, \quad \rho(r,z) = \frac{p^{\alpha}(r,z)}{k(r)},$$
$$\omega = \sqrt{\frac{p^{1-\alpha}}{\alpha - 1} \frac{k'(r)}{r}}.$$

2.4. Boundary conditions

The surface currents in the disk (at $z = 0$) lead to a discontinuity in the magnetic field disk-tangential components. Mathematically it means that the following condition is fulfilled (Landau & Lifshitz, 1982)

$$\boldsymbol{n} \times (\boldsymbol{B}^+ - \boldsymbol{B}^-) = \frac{4\pi}{c} \boldsymbol{i}, \tag{8}$$

where $\boldsymbol{B}^+$, $\boldsymbol{B}^-$ are the magnetic field under and over the disk respectively, $\boldsymbol{n}$ is the unit normal to the disk and directed downward in cylindrical coordinates. Since we suggest that MHD-flow is symmetric in relation to equatorial plane and consider the problem in the upper half-space, then $\boldsymbol{B}^+ = -\boldsymbol{B}^- = \boldsymbol{B}$ and (8) gives the following

$$\boldsymbol{n} \times \boldsymbol{B} + \frac{2\pi}{c} \boldsymbol{i} = 0. \tag{9}$$

Substituting expression for the surface current in the disk $\boldsymbol{i}$ which is due to the Ohm's law at the comoving frame $\boldsymbol{i} = -\lambda(\boldsymbol{u} - \boldsymbol{V}) \times \boldsymbol{B}/c$ into the equation (9) for current, finally we get

$$(\boldsymbol{u} - \boldsymbol{V} - \zeta \boldsymbol{n}) \times \boldsymbol{B} = 0. \tag{10}$$

Assuming that the angular velocity ω and r, φ-components of electric field in comoving frame change negligibly in z-direction on scales of the order of the disk thickness $2h$, we obtain for the disk surface electric conductivity $\lambda = \int \sigma_{\rm t} dz \sim 2h\sigma_{\rm t}$.

In spherical coordinates the tangential components of (10) are

$$\begin{aligned} &(v - V_{\rm k}) B_\theta - (w - \zeta) B_\varphi = 0, \\ &u B_\theta - (w - \zeta) B_R = 0. \end{aligned} \tag{11}$$

The relations (11), (expressing Ohm's law for surface current in the disk), give two boundary conditions in the equatorial plane under $\theta = \pi/2$ ($z = 0$).

The real disk has some vertical (in z-direction) structure that is not considered here. It is essential that thermodynamic parameters of the disk plasma change in the vertical direction turning smoothly to the corona ones. So, the boundary conditions can be set arbitrarily, based on some physically reasonable assumptions.

We assume that matter flows from the disk to the corona at small velocity. It could be expected that plasma leaves the disk with the velocity less than the slow magnetosonic one. Let us accept that the z-component of the velocity is a fraction α_c of the cusp one in this direction. The cusp velocity is not greater than slow magnetosonic one and has the same direction. The condition (12) guarantees that the plasma outflow does not exceed the slow magnetosonic one, giving the third boundary condition for $\theta = \pi/2$ ($\boldsymbol{a} = \boldsymbol{B}/\sqrt{4\pi\rho}$ is the Alfvén velocity, parameter $\alpha_c(R) < 1$):

$$w + \alpha_c(R) \frac{c_{\rm s} |a_\theta|}{\sqrt{c_{\rm s}^2 + a^2}} = 0. \tag{12}$$

The condition (12) guarantees also that from any point of the disk five characteristics come out. So, one should set another two boundary conditions.

We assume that matter outflow from the disk does not change its interior structure, i.e. the disk has sufficiently large mass, energy and angular momentum. We assume that the specific entropy of the matter flowing out from the disk does not vary with time

$$S\big|_{\theta=\pi/2} = S_d(R).$$

To get the equation describing the evolution of the magnetic flux function on the disk (at $\theta = \pi/2$) let us use the induction equation

$$\frac{\partial B_\theta}{\partial t} + \frac{c}{R} \frac{\partial R E_\varphi}{\partial R} = 0. \tag{13}$$

Taking into account that on the disk $B_\theta = \partial\Psi/(R\,\partial R)$ and Ohm's law is fulfilled, the azimuth component of the surface current, $E_\varphi + c\,B_R/(2\pi\sigma_t) = 0$. Integrating (13), we found

$$\frac{\partial \Psi}{\partial t} + \zeta R B_R = 0.$$

Let us formulate the boundary conditions on the inner bound of the simulation region under $R = R_{\rm in}$. As for boundary conditions on equatorial plane, they are set for reasons of physical rationality. The main factor to take into account is on the one hand to choose arbitrary the position of the inner bound, i.e. the value of the inner radius of the simulation region $R_{\rm in}$,

and, on the other hand, quickly (like R^{-6}) increasing magnetic pressure of stellar dipole-like field. $R_{\rm in}$ is chosen to be such that in some neighborhood of the inner bound, the star magnetic field has dominant influence on the plasma dynamics. In other words, in this region Alfvén velocity is much more than both the gas sound speed and the Keplerian one. On the other hand, the choice of a very small $R_{\rm in}$ is not reasonable from the computational point of view, because, into the simulation region, in this case includes parts of the magnetosphere where Alfvén velocity is too large. It leads to an essential decreasing of time integration step. Since in the considered model it is assumed that magnetic field lines are frozen into the star surface rotating with angular velocity Ω_*, on the inner bound of the simulation region (and under it, right on the star surface) plasma moves along the rotating magnetic field lines. In the frame of the rotating star (on inner bound) plasma velocity vector is parallel to the magnetic field one. Since transforming to the rotating frame $\boldsymbol{B}$ does not change, but $\boldsymbol{u}$ transforms into $\boldsymbol{u} - V_*\boldsymbol{e}_\varphi$, where $V_* = \Omega_* R_{\rm in}\sin\theta$. This boundary condition can be written in the following way ($R = R_{\rm in}$):

$$(\boldsymbol{u} - V_*\boldsymbol{e}_\varphi)\times\boldsymbol{B} = 0. \qquad (14)$$

Condition (14) implies also that in the rotating frame, the electric field in the inner bound is zero. The conditions (14) give two boundary conditions under $R = R_{\rm in}$.

On the outer bound, at $R = R_{\rm out}$, "free" boundary conditions are set. Such conditions should not influence on the solutions inside simulation region preventing poloidal magnetic field lines opening.

On the rotation axis, although it is not a bound, symmetry of the flow conditions for this axis are set:

$$v = w = 0,\ B_\varphi = B_\theta = 0,\ \Psi = 0 \ \text{ under } \ \theta = 0.$$

3. Numerical method and results

For the numerical integration of the ideal MHD equations (1), we use Godunov-type conservative high resolution scheme (Kulikovskii et al. 1999, Yelenina & Ustyugova 2004). To guarantee divergence–free magnetic field we apply the same procedure as Tóth (2000).

The system of equations (1) is integrated numerically in the region $R_{\rm in} < R < R_{\rm out}$, $0 < \theta < \pi/2$. We take a non-uniform grid in the radial direction, and uniform in the polar angle: $N_\theta = 60$, $N_R = 60$. The time step of the integration τ is restricted by Courant condition.

To verify the method and results we also used two grids: 120×60 and 240×120 and first order numerical method to estimate the numerical diffusivity of the scheme. To satisfy the goals of this paper, i.e. to investigate the regime of interaction between the magnetized star and the disk, it is turned out that the grid size presented in the paper is quite enough.

For mathematical simulation of the interaction between a magnetized star and its accretion disk we performed several runs for different surface magnetic diffusivity ζ. Fig. 2–7 present the results for the following values of parameter ζ: 0, 0.001, 0.005.

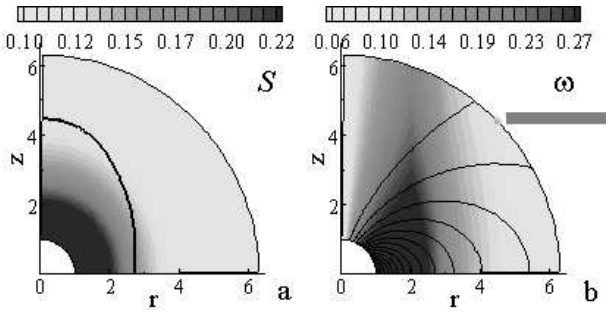

Fig. 2. (a) Background colour shows the initial distribution of the specific entropy $S(r,z)$, solid line presents the magnetic parameter $\beta = 1$. (b) Background colour shows the initial distribution of the angular velocity $\omega(r,z)$, thin lines present the magnetic flux function $\Psi(r,z)$.

Fig. 2 shows the initial system configuration at time moment, $t = 0$. The background color in Fig. 2a shows the plasma specific entropy distribution $S(r,z)$, thick line corresponds to the plasma parameter $\beta = 8\pi p/B^2 = 1$. The background color on Fig. 2b shows the plasma angular velocity distribution $\omega(r,z)$, streamlines show magnetic field lines – magnetic flux function $\Psi(r,z)$.

The evolution of the coronal magnetic field loops in the "star – disk" system depends on the surface magnetic diffusivity ζ. One can pick out the characteristic features which are essential for this process. For all the cases, poloidal field lines are pulled out and reconnected periodically (approximately each tenth rotation period of the disk inner bound). Then, a magnetic field toroidal component is generated. After reconnection, a plasmoid is formed. It is surrounded by closed poloidal magnetic field lines along which the poloidal electric current is running. Plasmoid is determined by a strong toroidal magnetic field and a low gas pressure. The angular velocity inside the plasmoid is different from the corona one. $t = 50$ is chosen for presenting the simulation results (the time is measured in disk inner bound rotation period). Up to that moment, several reconnections of magnetic field lines took place, and next ejected plasmoid moves outwards to the outer bound. Previous series of reconnections already led to the opening of the field lines close to the rotation axis. We should note that the reconnection of the magnetic field lines originates due to the numerical magnetic diffusivity. Nevertheless, we suppose that the reconnection and plasmoid ejection takes place as well for real magnetic diffusivity.

Fig. 3a–f show the distributions of some variables for a magnetic diffusivity $\zeta = 0$. The background colour on Fig. 3a shows the distribution of the poloidal current $J_p = R\sin\theta B_\varphi$. The magnetic field lines are shown also in this plot by firm lines. It is clear from these pictures that the initial configuration has essentially changed and now it is not dipole–like. In the disk differential rotation region ($r > 2$), field lines come out of its surface with large slope angle (more than 30°), fulfilling the conditions for matter outflow from the disk. A toroidal magnetic field is generated as a result of the differential rotation, implying that there is a poloidal current in the corona, forming a double current sheet (background dark colour area

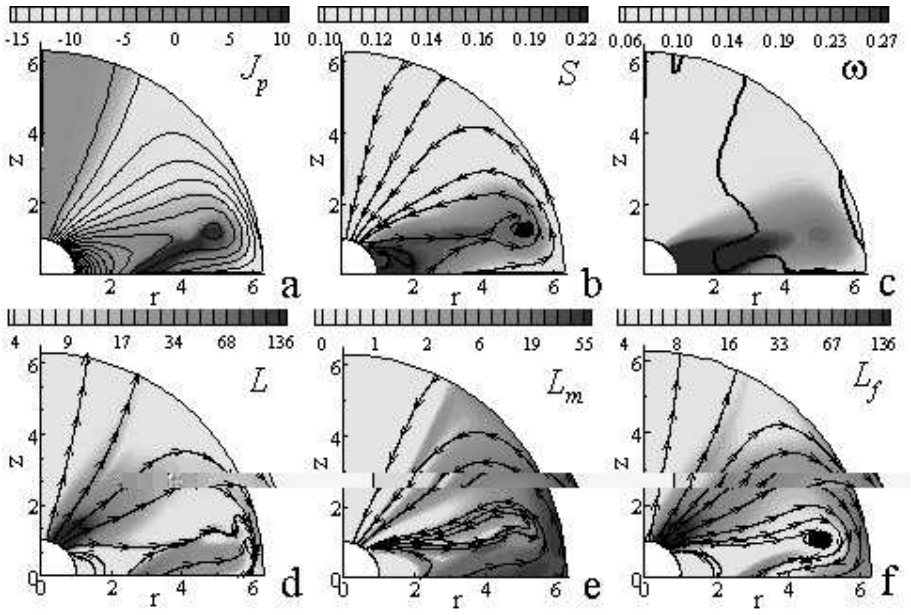

Fig. 3. Flow distributions for $\zeta = 0.0$ at $t = 50$. (a) Background colour shows the poloidal current J_p. The magnetic field lines are shown by firm lines. There is a poloidal current in the corona, forming a double current sheet (shown by background dark colour region). (b) Background colour shows the specific entropy S. Streamlines present the matter current lines. Plasmoid has hot matter surrounding it from the corona and moves up to the outer boundary. (c) Background colour shows the plasma angular velocity ω, firm line present the level of the plasma parameter $\beta = 1$. In the neighborhood of the star poloidal current lines approximately coincide with the poloidal field ones. Fig. (d)–(f) show the distribution of the angular moment transport in the system. (d) Background colour shows the magnitude of the angular momentum flux, and streamlines show the direction of the system angular momentum transport. (e) Streamlines show the angular momentum flux direction carried by matter. The background colour shows the magnitude of this vector. (f) Streamlines present the angular momentum flux direction, carried by the magnetic field, its magnitude is shown by colour. There are two regions of intense momentum transport. One of them is nearby the star pole where transport takes place due to magnetic stresses (f). The second one is above the disk, in the area of its differential rotation where the transport is caused by matter flow (e).

on Fig. 3a). In the neighborhood of the star poloidal current lines approximately coincide with the poloidal field ones.

The background colour on Fig. 3b shows the distribution of the specific entropy S. Streamlines present the matter current lines. It is clear that the matter flows into the plasmoid area from the star and the disk inner part. Plasmoid has hot matter surrounding it from the corona and moves up to the outer boundary.

The background colour on Fig. 3c shows the plasma angular velocity distribution, firm line – plasma parameter level $\beta = 1$. It is evident from comparing Fig. 3a and Fig. 3c that the angular velocity is practically constant along the field lines, especially nearby the star. It means that in this area the generation of the toroidal magnetic field does not take place, i.e. there are no poloidal electric currents. The magnetosphere, rotating with constant angular velocity, gives angular momentum to the plasmoid, twisting the matter inside it.

Fig. 3d – 3f show the distributions of several quantities that describe the angular moment transport in the system. The angular momentum conservation equation can be found from the continuity equation and is

$$\frac{\partial \rho l}{\partial t} + \mathrm{div}\boldsymbol{L} = 0,$$

here $\rho l = \rho u R \sin\theta$ is the angular momentum density. The poloidal components of the angular momentum flux density are

$$\boldsymbol{L} = R\sin\theta\left(\rho v \boldsymbol{u}_p - \frac{B_\varphi \boldsymbol{B}_p}{4\pi}\right),$$

where $\boldsymbol{u}_p$, $\boldsymbol{B}_p$ are the plasma poloidal velocity and the poloidal magnetic field. The first term in the right part describes angular momentum transported by matter, the second one does by magnetic field.

The background colour on Fig. 3d shows the magnitude of the angular momentum flux, and streamlines show the direction of the system angular momentum transport. There are two areas of intense momentum transport. One of them is nearby the star pole where transport takes place due to magnetic stresses (see Fig. 3f). The second one is above the disk, in the area of its differential rotation where the transport is caused by matter flow. These processes are presented on Fig. 3e,f in more detail. On Fig. 3e, streamlines show the angular momentum flux direction carried by matter. The background colour shows the magnitude of this vector. On Fig. 3f streamlines – angular momentum flux direction, carried by the magnetic field, by colour – its magnitude. It is clear from the Fig. 3f that angular momentum from the star is transported by magnetic field mainly. Also there is intense momentum transport inside the plasmoid.

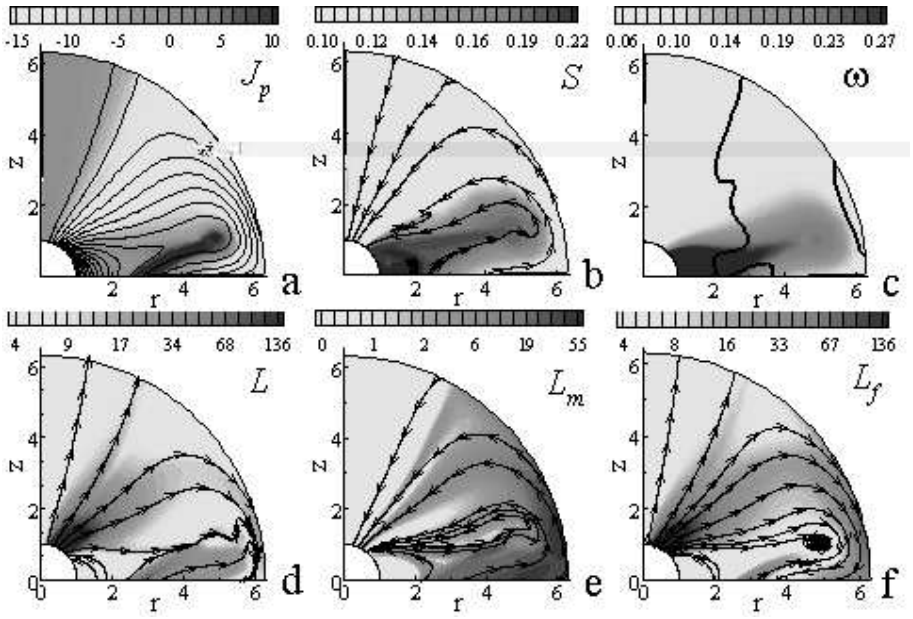

Fig. 4. Flow distributions for $\zeta = 0.001$ at $t = 50$. (a) Background colour shows the poloidal current J_p. The magnetic field lines are shown by firm lines. (b) Background colour shows the specific entropy S. Streamlines present the matter current lines. (c) Background colour shows the plasma angular velocity ω, firm line presents the plasma parameter level $\beta = 1$. Fig. (d)–(f) show the distribution of the angular moment transport in the system. (d) Background colour shows the magnitude of the angular momentum flux, and streamlines show the direction of the system angular momentum transport. (e) Streamlines show the angular momentum flux direction carried by matter. The background colour shows the magnitude of this vector. (f) Streamlines show the angular momentum flux direction, carried by the magnetic field, its magnitude is presented by colour.

The distributions for the same variables at $t = 50$ are shown on Fig. 4–5 in case of a finite surface magnetic diffusivity. Fig. 4a–4f correspond to $\zeta = 0.001$, Fig. 5a–5f – $\zeta = 0.005$.

The Fig. 6a–c show the influence of the magnetic diffusivity on the magnetic field topology. Level lines of the magnetic flux function $\Psi(r, z)$ for all cases (a: $\zeta = 0$, b: $\zeta = 0.001$, c: $\zeta = 0.005$) are chosen at $t = 11$. At this time, the first reconnection took place for the case $\zeta = 0$. It is clear (see Fig.6a–c) that the less the disk conductivity (i.e. the more magnetic diffusivity), the more the distance from the axis and the disk where the plasmoid ejection takes place. In case of imperfect disk conductivity, field lines are no longer frozen into the disk and, twisted by the star, they are shifted outwards. We can say that the more the surface magnetic viscosity ζ, the slower the evolution takes place, and the more seldom plasmoids are formed in corona.

The matter flowing out from the disk and the magnetic field both take away the angular momentum from it. The whole angular momentum flux taken away from the disk per unit time is

$$L = L_m + L_f = -\int \rho(\boldsymbol{r}\times\boldsymbol{u})\boldsymbol{u}d\boldsymbol{S} + \frac{1}{4\pi}\int(\boldsymbol{r}\times\boldsymbol{B})\boldsymbol{B}d\boldsymbol{S}.$$

Here, the integration is over the disk surface, $d\boldsymbol{S}$ is the element of disk surface directed outwards (from the simulation region). The first term L_m is the angular momentum flux carried by matter, the second one L_f is the angular momentum flux carried by magnetic field.

The time dependence of the angular momentum fluxes carried by matter L_m, by magnetic field L_f and their sum $L = L_m + L_f$ are shown on Fig. 7a–c for different values of ζ.

For $\zeta = 0$ (see Fig. 7a), the process of angular momentum transport from the disk to the corona is quasi-periodic with period equal approximately to ten rotation periods of the disk inner part. After $t_* = 45$ there is relaxation of the system accompanied by small oscillations of the angular momentum fluxes. During this time there no new plasmoids are generated. After $t = 65$, the reconnection process of the magnetic field lines is resumed. It can be seen from the angular momentum fluxes oscillations (see Fig. 7a).

The finite disk conductivity changes the course of events (interaction between magnetic star and accretion disk). As it is seen from Fig. 7a–c, the magnetic lines reconnection lasts until some time t_* (depending on ζ). The more the magnetic diffusivity ζ, the later the plasmoids ejection begins and the earlier ends. We should note that in case of an imperfect disk conductivity the coronal magnetic field evolution is qualitative similar to the perfect one. The reconnection of magnetic field lines takes place at the time corresponding to the maximum angular momentum outflow carried by magnetic field from the disk. In contrast to a perfect disk conductivity ($\zeta = 0$), the activity of the reconnection slows down and the system relaxes to such a state that no new plasmoids are generated. The disk angular momentum carried by magnetic field gets balanced by angular momentum carried by matter. Non-frozen in the disk magnetic field lines move along the disk and it lead to the increasing of the magnetic flux in the disk.

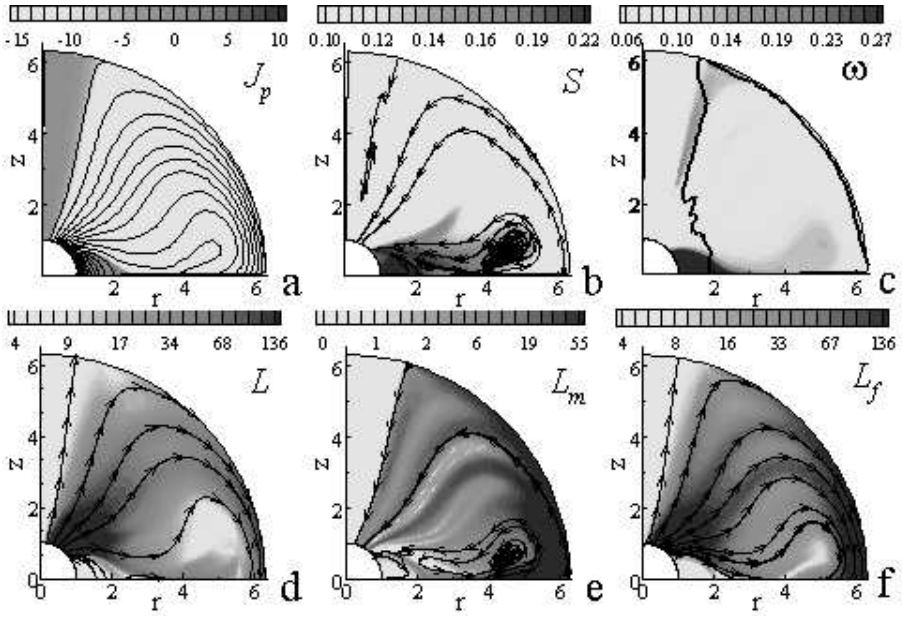

Fig. 5. Flow distributions for $\zeta = 0.005$ at $t = 50$. (a) Background colour shows the poloidal current J_p. The magnetic field lines are shown by firm lines. (b) Background colour shows the specific entropy S. Streamlines present the matter current lines. (c) Background colour shows the plasma angular velocity ω, firm line presents the plasma parameter level $\beta = 1$. Fig. (d)–(f) show the distribution of the angular moment transport in the system. (d) Background colour shows the magnitude of the angular momentum flux, and streamlines show the direction of the system angular momentum transport. (e) Streamlines show the angular momentum flux direction carried by matter. The background colour shows the magnitude of this vector. (f) Streamlines show the angular momentum flux direction, carried by the magnetic field, its magnitude is presented by colour.

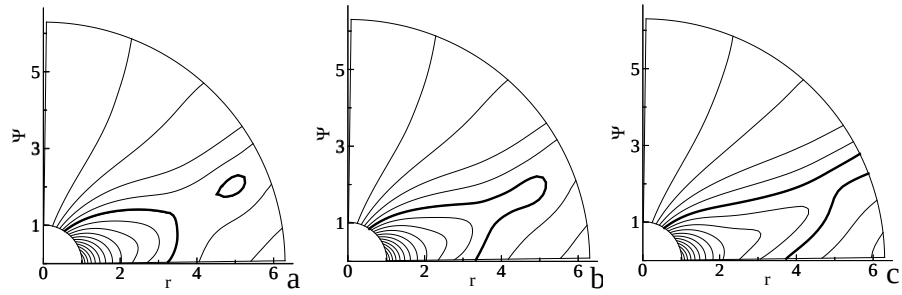

Fig. 6. (a)–(c) Influence of the surface magnetic diffusivity ζ on the magnetic field topology at $t = 11$ when the first reconnection took place for the case $\zeta = 0$. Level lines of the magnetic flux function $\Psi(r, z)$ are shown by thin lines (magnetic field lines: on (a) for $\zeta = 0.0$, on (b) for $\zeta = 0.001$, on (c) for $\zeta = 0.005$, $\Psi = 151.6$ is shown by solid line. The more the magnetic diffusivity, the more the distance from the axis and the disk where the plasmoid ejection takes place. In case of imperfect disk conductivity, field lines are no longer frozen into the disk and are shifted outwards.

4. Summary and conclusions

The influence of the disk surface magnetic diffusivity on the "star–corona–disk" system evolution was studied. For all the cases, poloidal field lines are pulled out and are reconnected periodically approximately each tenth rotation period of the disk inner bound. The magnetic field configuration has essentially changed from initially dipole-like one. The magnetic field lines come out of its surface with large slope angle, fulfilling the conditions for matter outflow from the disk, in the disk differential rotation region.

The more the magnetic diffusivity, the more the distance from axis and disk where the plasmoid ejection takes place. In the case of imperfectly disk conductivity, magnetic field lines are no longer frozen into the disk and, twisted by the star, they are shifted outwards. The more surface magnetic diffusivity ζ, the slower the evolution takes place and more seldom plasmoids are formed in corona.

In the case of an imperfectly disk conductivity, the coronal magnetic field evolution is qualitative similar to the perfect one. The reconnection of magnetic field lines takes place at the time corresponding to the maximum angular momentum outflow carried by magnetic field from the disk. In contrast to a perfect disk conductivity, the activity of the reconnection slows down and the system relaxes to such a state that no new plasmoids are generated. The disk angular momentum carried by

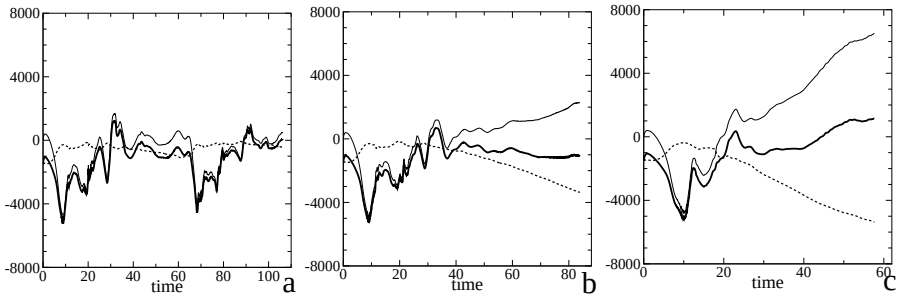

Fig. 7. Time dependence of the angular momentum fluxes carried by matter L_m, by magnetic field L_f and total $L = L_m + L_f$ for different ζ: on (a) for $\zeta = 0.0$, on (b) for $\zeta = 0.001$, on (c) for $\zeta = 0.005$; L_m is shown by dashed line, L_f is shown by thin line, L is shown by solid line. For $\zeta = 0$ (a), the process of angular momentum transport from the disk to the corona is quasi-periodic with period equal approximately to ten rotation periods of the disk inner part. Then, after the relaxation the process is resumed. For $\zeta = 0.001$ (b) and $\zeta = 0.005$ (c), the magnetic lines reconnection lasts until some time. The more the magnetic diffusivity ζ, the earlier the plasmoids ejection ends. The reconnection of magnetic field lines takes place at the time corresponding to the maximum angular momentum outflow carried by magnetic field from the disk. In contrast to a case for $\zeta = 0$, the activity of the reconnection slows down and the system relaxes to such a state that no new plasmoids are generated. The disk angular momentum carried by magnetic field gets balanced by angular momentum carried by matter, in particular, $|L| \ll |L_f|$.

magnetic field gets balanced by angular momentum carried by matter. Non-frozen in the disk magnetic field lines move along the disk and it leads to the increasing of the magnetic flux in the disk.

Summing up we can give following conclusions.

1. In the case of perfectly conducting disk the evolution of the coronal magnetic field leads to quasi-periodic outflow of the angular momentum from the disk. The interaction process occurs with the reconnection of the magnetic field lines and plasmoid ejections.
2. In the case of imperfectly conducting disk the configuration of the magnetic field lines is formed such that the angular momentum flux carried by the magnetic field from the disk becomes balanced by the flux transported by matter.

Acknowledgements. Part of this work was supported by the *Russian Foundation of Basic Research, RFBR* project number 06-02-16608, *Scientific School Program* project number 9399.2006.2 and *RAS Presidium Program* number 14.

References

Balbus, S.A. 2003, ARA&A, 41, 555
Bisnovatyi–Kogan, G.S.,& Lovelace, R.V.E. 2001, New Astron. Rev., 45, 663
Blandford, R.D.,& Payne, D.G. 1982, MNRAS, 199, 883
Fendt, C.,& Čemeljić, M. 2002, A&A, 395, 1045
Fendt, C.,& Elstner, D. 1999, A&A, 349, L61
Fendt, C.,& Elstner, D. 2000, A&A, 363, 208
Ferreira, J. 1997, A&A, 319, 340
Hawley, J.F., Gammie, C.F.,& Balbus, S.A. 1995, ApJ, 440, 742
Hayashi, M.R., Shibata, K.,& Matsumoto, R. 1996, ApJ, 468, L37
Krasnopolsky, R., Li, Z.-Y.,& Blandford, R. 1999, ApJ, 526, 631
Kulikovskii, A.G., Pogorelov N.V.,& Semenov, A.Yu. 1999, Mathematical Aspects of Numerical Solution of Hyperbolic Systems, Monographs and Surveys in Pure and Applied Mathematics. (Chapman and Hall/CRC, Boka Raton, FL) 598
Kuwabara, T., Shibata, K., Kudoh, T.,& Matsumoto, R. 2000, PASJ, 52, 1109
Landau, L.D.,& Lifshitz, E.M. 1982, Electrodynamics of Continuous Media. Volume VIII (Nauka, Moscow) 620
Ouyed, R.,& Pudritz, R.E. 1997, ApJ, 482, 712
Romanova, M.M., Ustyugova, G.V., Koldoba, A.V.,& Lovelace, R.V.E 2002, ApJ, 578, 420
Shakura, N.I.,& Sunyaev, R.A. 1973, A&A, 24, 337
Shu, F., Najita, J., Ostriker, E., Wilkin, F., Ruden, S.,& Lizano, S. 1994, ApJ, 429, 781
Tóth, G. 2000, J. Comput. Phys., 161, 605
Ustyugova, G.V., Koldoba, A.V., Romanova, M.M., Chechetkin, V.M.,& Lovelace, R.V.E 1999, ApJ, 516, 221
Uzdensky, D.A. 2004, Ap&SS, 292, 573
Yelenina, T.G.,& Ustyugova, G.V. 2004, Prepint KIAM RAS, No 73